Environmental Science & Technology

Article

Cite This: Environ. Sci. Technol. 2019, 53, 12054−12061

pubs.acs.org/est

Chemical Composition and Toxicity of Particles Emitted from a Consumer-Level 3D Printer Using Various Materials

Qian Zhang,[†,⊥] Michal Pardo,[‡,⊥] Yinon Rudich,[‡] Ifat Kaplan-Ashiri,[○] Jenny P. S. Wong,[∥] Aika Y. Davis,[†] Marilyn S. Black,[†] and Rodney J. Weber*[,∥]

[†]Chemical Safety and Human Health, Underwriters Laboratories Inc., Marietta, Georgia 30067, United States

[‡]Department of Earth and Planetary Sciences and [○]Department of Chemical Research Support, Weizmann Institute of Science, Rehovot 76100, Israel

[∥]School of Earth and Atmospheric Sciences, Georgia Institute of Technology, Atlanta, Georgia 30332, United States

Supporting Information

ABSTRACT: Consumer-level 3D printers emit ultrafine and fine particles, though little is known about their chemical composition or potential toxicity. We report chemical characteristics of the particles in comparison to raw filaments and assessments of particle toxicity. Particles emitted from polylactic acid (PLA) appeared to be largely composed of the bulk filament material with mass spectra similar to the PLA monomer spectra. Acrylonitrile butadiene styrene (ABS), extruded at a higher temperature than PLA, emitted vastly more particles and their composition differed from that of the bulk filament, suggesting that trace additives may control particle formation. In vitro cellular assays and in vivo mice exposure all showed toxic responses when exposed to PLA and ABS-emitted particles, where PLA-emitted particles elicited higher response levels than ABS-emitted particles at comparable mass doses. A chemical assay widely used in ambient air-quality studies showed that particles from various filament materials had comparable particle oxidative potentials, slightly lower than those of ambient particulate matter ($PM_{2.5}$). However, particle emissions from ABS filaments are likely more detrimental when considering overall exposure due to much higher emissions. Our results suggest that 3D printer particle emissions are not benign and exposures should be minimized.

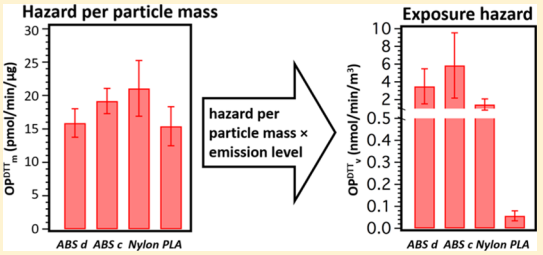

1. INTRODUCTION

Three-dimensional (3D) printing is an emerging technology in industrial applications but also popular for domestic usage.[1] Fused filament fabrication 3D printing heats a thermoplastic material and deposits it by layers to build an object. Among a wide range of materials, acrylonitrile butadiene styrene (ABS) and polylactic acid (PLA) are commonly utilized filaments. ABS is characterized by high strength, stiffness, and resistance to chemicals. It also requires higher extruder nozzle and build-plate temperatures than PLA.[2] PLA is biodegradable, thermally unstable, and more brittle compared to other plastics.[2] Numerous studies show that 3D printing emits both particles and volatile organic compounds (VOCs); emissions can depend on many factors, such as printer brand, filament material, filament brand and color, extrusion temperature, and filament feed rate.[3−9] Previous studies on laser printers and thermal processing of plastics showed potential exposure to gases and particles,[10,11] suggesting that 3D printer emissions may also be of concern.[12] While it was shown that 3D printers emit potentially harmful VOCs like styrene, caprolactam, ethylbenzene, and others,[3,13,14] particle chemical speciation is not well characterized, and the toxicity is also uncertain. To date, most of particle composition measurements reported have focused on organic compounds and metals.[9,13,15−17]

Measurements show that the average particle emission rates during 3D printing range from 2×10^8 to 2×10^{12} min^{-1},[3,5−9,15,17,18] and most of the emitted particles are ultrafine (less than 0.1 μm diameter).[6,7,9] Ultrafine particles are potentially harmful because they can deposit in the respiratory tract, enter the blood stream, translocate to remote organs, and damage mitochondria because of their specific properties.[19−21] A well-established mechanism associated with particle adverse biological effects, for both nanoparticles (NPs)[22] and ambient fine particles,[23] is the generation of reactive oxygen species (ROS), the excess of which causes cellular damage and induces oxidative stress.[24−26] Oxidative stress can trigger redox-sensitive pathways that lead to biological responses, such as inflammation,[22,27] cell death,[28] and diseases.[23,24] One integrative measure of a particle ability to induce oxidative stress is the particle oxidative potential (OP), which has been measured by various acellular assays.[29−32] The OP of ambient $PM_{2.5}$ (PM smaller than 2.5 μm in size) has been linked to adverse health effects associated

Received: July 12, 2019
Revised: September 10, 2019
Accepted: September 12, 2019
Published: September 12, 2019

DOI: 10.1021/acs.est.9b04168
Environ. Sci. Technol. 2019, 53, 12054−12061

with acute cardiorespiratory outcomes in a large metropolitan environment.[30,33−36]

In light of the emerging applications of consumer 3D printers and the potential increase in the exposure to the emitted particles, this study focuses on chemical composition and potential health impacts of particles emitted during 3D printing. Specifically, we analyze particle chemical composition via multiple methods and compare with the raw filament material. We also assess particle toxicity through the in vivo inflammatory model and in vitro cellular and acellular models through oxidative stress mechanisms and estimate potential exposure during printing.

2. METHODS

2.1. Particle Preparation and Characterization. *2.1.1. Particle Sample Preparation.* A consumer-grade 3D printer was operated in a 1 m^3 well-mixed stainless-steel emission test chamber.[7] Air removed of particles and VOCs via a high-efficiency particulate air filter (Pall Corporation, Port Washington, NY, USA) and an absorption column[37] was supplied to the chamber continuously, resulting in an air exchange rate of one volume per hour. Three filament materials were tested using the same 3D printer; two ABS filaments (hereafter denoted as *ABS c* and *d* for consistency with earlier work[7,38]) and a PLA filament (hereafter *PLA*). A nylon filament (hereafter *Nylon*) was tested with only the dithiothreitol (DTT) assay (Section 2.3). The tested printer extruder temperature was 270 °C for ABS, 210 °C for PLA, and 243 °C for nylon. Build-plate temperature was 100 °C for ABS and nylon and 50 °C for PLA. Particle concentrations in the chamber were monitored with online particle measurement instrumentation including a condensation particle counter (CPC 3022A, TSI Inc., Shoreview, MN, USA), a scanning mobility particle sizer (differential mobility analyzer 3081 and CPC 3785, TSI Inc.), and an optical particle counter (AeroTrak 9306-01, TSI Inc.), collectively measuring particle number concentrations as a function of size for particles spanning nominally 7 nm to 25 μm in diameter. Surface area and mass (volume) concentrations were calculated from the measured number distributions, assuming that particles were spheres of unit density. These calculated values are not necessarily the true particle surface area and mass because particle shape and density are not known; an estimation of the resulting uncertainties can be found in Zhang et al. 2017.[7]

In addition, particles for offline toxicity analysis were collected on 25 mm laminated polytetrafluoroethylene (PTFE) membrane filters with 0.45 μm pore size (Sterlitech Corporation, Kent, MA, USA) throughout the printing period. The sampling flow rate was 10 L/min, and the sampling time (i.e., printing period) varied to collect sufficient mass on the filter (Tables S1 and S2). Typical background number concentrations in the chamber were less than nominally 5 cm^{-3}. The aqueous particle suspensions for toxicity analyses were prepared by extracting each filter in deionized water (DI water) via sonication. The particle concentrations in the liquid samples were estimated as described in the Supporting Information S1.1 for the biological toxicity analyses (Figure S1 and Table S1) and in S1.2 for the chemical analysis (Table S2).

2.1.2. Particle Chemical Characterization. For *ABS c*- and *PLA*-emitted particles, submicron particle chemical composition (e.g., nonrefractory organic species and inorganic species, such as sulfate, nitrate, and ammonia) was measured online from the chamber by either an aerosol chemical speciation monitor (ACSM, Aerodyne Research, Inc., Billerica, MA, USA)[39] or a time-of-flight aerosol mass spectrometer (AMS, Aerodyne Research, Inc.)[40,41] during the printing period. For *ABS d*, pyrolysis gas chromatography mass spectrometry (GC−MS, Agilent Technologies, Santa Clara, CA, USA) was performed on both the filament and the emitted particles collected on a quartz filter. Although this method is not optimal for aerosol composition measurements because of limitations with filter sampling and sample alteration during pyrolysis, the goal was to directly contrast the composition of filament and particles generated from that filament with the same instrument.

2.1.3. Scanning Electron Microscope. Scanning electron microscope (SEM) imaging was applied to assess the solubility of particles (i.e., whether they remained solid in very dilute aqueous solution) and to roughly compare particle properties in liquid samples to those in situ. The filters and particle suspensions were prepared in the same way as for biological toxicity analyses. The samples were coated with 8 nm thick carbon using the Safematic CCO-010 HV high-vacuum coater and analyzed by Zeiss Ultra55 high-resolution SEM. The landing voltage was 3−5 kV, and images were recorded using the in-lens detector (high resolution topography contrast).

2.2. In Vitro Cellular Assays. *2.2.1. Cell Culture.* Rat alveolar macrophages (NR8383, CRL 2192) and human tumorigenic lung epithelial cells (A549), which represent the interaction with particles in lungs, were used to assess cytotoxicity of the particles and to compare the potential different responses because of their specific properties and functions. NR8383 cells were grown in Hams F12K medium (Biological Industries, Beit-Haemek, Israel) supplemented with 15% (w/v) fetal calf serum, 1% (w/v) glutamine, and 1% (w/v) penicillin−streptomycin. A549 cells were grown in RPMI-1640 supplemented with 10% (w/v) fetal calf serum and 1% (w/v) penicillin−streptomycin. Both cultures were incubated at 37 °C in a humidified atmosphere consisting of 95% air and 5% CO_2.

2.2.2. WST-1 Cell Viability Assay. Cell viability was evaluated by the WST-1 (Abcam, UK) assay 24 h after exposure, according to the manufacturer instructions and as previously described.[42] Cells were seeded 24 h prior to exposure. All samples were sonicated in a water bath for 5 min and then buffered with salts glucose media (pH = 7.2) prior to use, which comprised 50 mM Hepes, 100 mM NaCl, 5 mM KCl, 2 mM $CaCl_2$, and 5 mM glucose. Exposure was done using original extracted particle suspensions and 10-time diluted suspensions. Absorbance of the samples was measured at 440 and 650 nm by a microplate reader (BioTek, USA). Each experiment was repeated twice in quadruplicates for each cell type.

Cell death mechanism and intracellular ROS generation were also studied using original particle suspensions, details of those methods can be found in the Supporting Information section S2.

2.3. DTT (dithiothreitol) acellular Assay. OP of 3D printer-emitted particles was assessed using the DTT cell-free assay, following the method in Cho et al.[43] For DTT assay tests on water-soluble particles, the filter was extracted in 4.9 mL of DI water by sonication for 1 h, the extract was filtered through a 0.45 μm PTFE syringe filter (Fisher Scientific, USA), and then analyzed using a semiautomated DTT analytical system.[29] In brief, the sample was incubated with

DOI: 10.1021/acs.est.9b04168
Environ. Sci. Technol. 2019, 53, 12054−12061

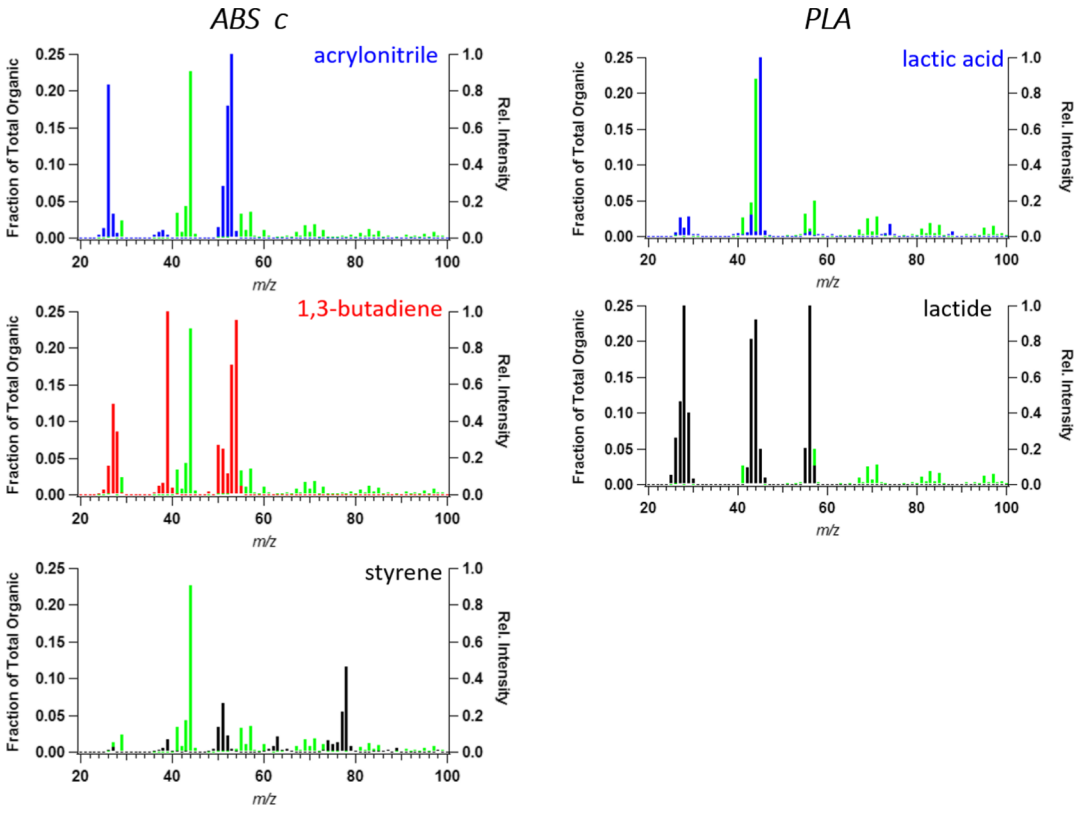

Figure 1. Online chemical composition measurements (with an ACSM) of particles emitted from filament *ABS c* and *PLA*. Particle mass spectra are shown in green. Reference spectra of monomers corresponding to the raw filament materials for ABS (acrylonitrile, blue; 1,3-butadiene, red; styrene, black) and PLA (lactic acid, blue; lactide, black) are included for comparison.[45]

DTT and potassium phosphate buffer at 37 °C and pH of 7.4. At five designed time points, the absorbance of the colored product from DTT reacting with 5,5′-dithiobis-(2-nitrobenzoic acid) was measured at 412 nm, which was used to determine the remaining DTT. For DTT assay tests on total particulates (i.e., soluble + insoluble), the analysis was similar to the water-soluble DTT assay, except the sample filter was kept in direct contact with DTT during incubation (i.e., no filtration of extract), following Gao et al.[44] Blanks (i.e., extracts of blank filters) and positive controls (9,10-phenanthrenequinone) were also carried out in the same manner. DTT concentrations were quantified based on a predetermined absorbance calibration curve using standard DTT solutions. For each sample, the DTT consumption rate was obtained by a linear fitting of the five points of remaining DTT. OP can be expressed as DTT consumption (corrected by blank) normalized by particle mass (OP_m^{DTT}) or sample air volume (OP_v^{DTT}).[29] A measurement was considered above the detection limit when the signal was larger than three times the standard deviation of the blanks. Particle concentration in the extract for total DTT analysis was based on particle mass collected on the filter and the volume of the extraction liquid (see Supporting Information section S1.2 for details).

2.4. Statistical Analysis. The differences between treatment groups were analyzed by one-way analysis of variance and considered significant at $p < 0.05$ using the Fisher-protected least-significant difference method. The *t* tests were used to compare the results of two different groups at a *p*-value of 0.05.

3. RESULTS AND DISCUSSION

3.1. Characterization of 3D Printer-Emitted Particles. *3.1.1. Particle Emission.* Detailed descriptions of emissions and contrasts between particle numbers and sizes for these (and many other) filaments can be found in Zhang et al.[7] In general, particles emitted from all filaments were lognormally distributed (Figure S2). Time series of total particle number, surface ,and volume (mass) concentrations are given in Figure S3. Particle number emission yields (total particle number emitted per mass of object printed) for the filaments tested (examples are shown in Figures S2 and S3) were as follows: *ABS d* 1.42×10^{11} g^{-1}, *ABS c* 1.52×10^{10} g^{-1}, *PLA* 1.35×10^{9} g^{-1}, and *Nylon* 1.58×10^{9} g^{-1}. Estimated particle surface area and volume (mass) yields and mean particle sizes can be found in Table S3.

3.1.2. Particle Chemical Composition. The ACSM can quantify nonrefractory organic and inorganic species. The results showed that the particles emitted from *ABS c* and *PLA* filaments were largely organic in composition; inorganic species were below limit of detection (LOD). Other trace species, such as metals, may be present[17] but were not measured in this study. ACSM data also showed that the mass spectra of *ABS c* and *PLA* emitted particles were different, indicating their compositions differed, as expected (Figure 1). Furthermore, the mass spectra of *ABS c* emitted particles were different from those of the raw filament material monomers (i.e., acrylonitrile, 1,3-butadiene, styrene),[45] whereas the mass spectra of *PLA*-emitted particles were mostly similar to those of the PLA monomers (i.e., lactic acid, lactide) (Figure 1). This is consistent with Vance et al.,[16] where the Raman spectra of ABS-emitted particles lacked the peaks corresponding to

DOI: 10.1021/acs.est.9b04168
Environ. Sci. Technol. 2019, 53, 12054−12061

ABS monomers seen in the spectra of ABS filament. Additionally, for *ABS c*-emitted particles, no significant change in the mass spectra (measured by the AMS) was observed throughout the print time (Figure S4), suggesting that these particles were not subjected to additional processing following their emission (i.e., evaporation of semivolatile components, reactions with oxidants). However, for *PLA*-emitted particles, the fraction of small organic fragments [mass to charge (m/z) < 30] increased throughout print time (Figure S4). While we cannot identify the chemical species leading to the observed changes, because of the similarity in the mass spectral pattern of this group of small m/z fragments to lactic acid (Figure 1), we speculate that the increasing contribution of lactic acid to particle composition is because of the increasing total particle surface area throughout the print time, which increases the partitioning of semivolatile organic gases emitted from PLA.

Because the ACSM/AMS does not allow for the analysis of filament composition, pyrolysis GC−MS provided a more direct comparison of composition between the filament material and the particles formed. Focusing on ABS filaments, because the particles appeared to be chemically different from the filament, the evolved gas analysis of *ABS d*-emitted particles confirmed that they had substantially different spectra from that of the *ABS d* raw filament (Figure S5), both measured by the same instrument. This indicated that the ABS particles are not formed mainly from the bulk ABS filament material but potentially from some additives, such as fatty acids (Figure S5) and plasticizers or antioxidants.[9]

To some degree, the chemical analysis can help explain contrasts in emissions from the two ABS filaments tested and differences between PLA and ABS in general. For ABS, apparently, a minor unknown filament additive accounts for the particle formation, which was consistent with previous model results.[38] Different additives may be used by different filament manufacturers, for example, *ABS d* that had much higher particle emissions contained 5−10% more additives than *ABS c*, according to the safety sata sheets from the manufacturers. (Specific chemical details of the additives are not provided). *PLA* is printed at a much lower temperature, therefore in general, PLA may be less susceptible to volatilization of typical filament additives, leading to the bulk material mainly contributing to the particle formation, and much lower particle emissions. (Note, there is data showing PLA filaments with specialized properties, which contain additional unknown additives, can also be much higher aerosol emitters than regular PLA filaments, consistent with this line of reasoning).[7] Our findings on the particle chemistry imply that the toxicity of particles emitted from 3D printers could vary widely amongst filaments on the market and may not be directly related to the toxicity of the bulk filament materials.

3.1.3. Particle Imaging Analysis. Though changes in particle characteristics may occur during the processing, SEM images of dried particle suspensions (Figure S6) provided information on particle shape, size, and morphology. Particle diameters estimated roughly from SEM images were 71 ± 20 nm (mean ± standard deviation) for *ABS d*, 106 ± 20 nm for *ABS c*, and 14 ± 25 nm for *PLA*. Sizes were estimated from the images by analysis of 15 particles for *PLA* and 50 particles for both *ABS*. Because of the much smaller size of *PLA* particles, this method of sizing was highly uncertain. The SEM analysis showed that the particle sizes in the aqueous samples were comparable to those measured in the chamber during filter sampling (Table S3, mean sizes for the number distributions were 49, 123, and 51 nm for *ABS d*, *ABS c*, and *PLA*, respectively). Imaging also indicated that the particles were not highly water-soluble as they were in solution for an extended period of time (over 30 days) prior to SEM analysis and remained (or at least some fraction remained) as detectible solid particles.

3.2. Cytotoxicity of Particles. Human tumorigenic bronchial epithelial cells (A549) represent respiratory cells that could be affected by inhalation exposure, and rat alveolar macrophages (NR8383) represent cells defending against invasion to lungs. The effects of 3D printer-emitted particles on cell viability of these two cell types were measured by the WST-1 assay 24 h after exposure and are shown in Figure 2.

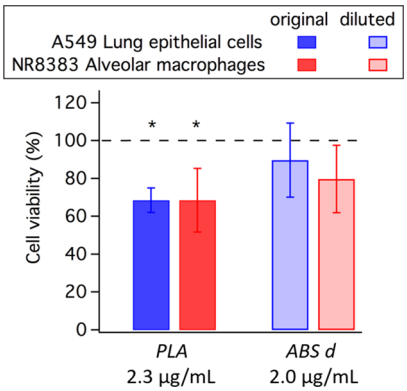

Figure 2. Cell viability results from the WST-1 assay for *PLA* and *ABS d* samples at indicated concentrations on the two cell types. Error bar represents standard deviation; asterisk indicates a significant (p < 0.05) difference from the blank. Sample concentrations are given on the plot. Note that the *ABS d* sample had to be diluted 10 times to provide a similar dose because of its much higher emission rate.

The cell viability after exposure to *PLA*-emitted particles reduced statistically significant compared to cells exposed to blanks for both cell types (Figure 2). However, exposure to *ABS d*-emitted particles at a similar dose did not induce statistically significant decrease in cell viability for either cell types (Figure 2). This indicated PLA-emitted particles may be more toxic when exposed to comparable doses for the selected cell types.

Additional cellular assays and in vivo exposure experiments were performed to test if the particles were benign. Although not at similar doses, thereby limiting direct contrasts between filament types, both these filaments showed toxic responses over blanks, indicating the potential toxicity of 3D printer-emitted particles to living cells and mice immune system, and details of the results can be found in the Supporting Information section S4 (Figures S7−S11).

3.3. Oxidative Potential Measured by DTT Assay. Results for the cell-free DTT assay showed that the water-soluble OP was below LOD, while the total particle OP was above LOD, for all the particles tested (*ABS d*, *ABS c*, *PLA* and *Nylon*). This was also consistent with the SEM result that showed particles were nominally water insoluble (Figure S6), thus a null result for soluble species is expected. A set of filters were collected for total (soluble + insoluble species) DTT analysis, where the mass collected on the filters was controlled to be within a difference of 2% (see Supporting Information Table S2), such that the exposure doses (i.e., particle concentrations in samples) were at similar levels. As shown

DOI: 10.1021/acs.est.9b04168
Environ. Sci. Technol. 2019, 53, 12054−12061

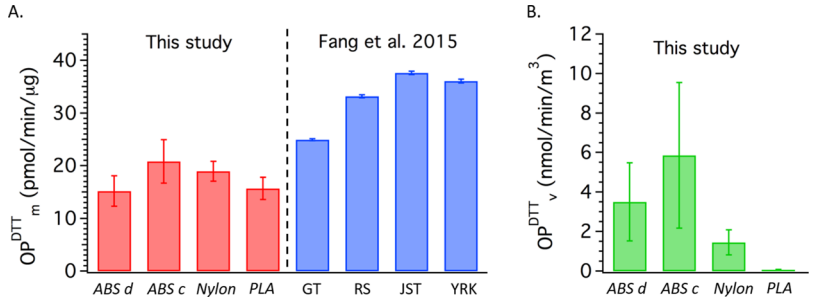

Figure 3. (A) OP^{DTT}_m measured by the total DTT assay method for the four particle samples, compared to OP^{DTT}_m of ambient air $PM_{2.5}$ results from different monitoring sites.[29] (B) OP^{DTT}_v measured by total DTT assay for the four particle samples based on the chamber setup in this study. The error bar for this study represents standard deviation of repeated measurements (n = 3 for each filament sample) and the error bar for Fang et al.[29] represents standard deviation of data for each monitoring site. GT was a site at the Georgia Institute of Technology; RS was a roadside site close to 75/85 interstate in midtown Atlanta; JST was an urban site at Jefferson Street, Atlanta; YRK was a rural site in Yorkville, GA considered to be generally upwind of Atlanta.

in Figure S12, all four particle samples analyzed showed statistically significant higher responses than blanks. Small variability was observed across the means but not statistically significant between any two sample groups.

Because a large data set exists for the OP^{DTT} of ambient aerosols and emissions from a wide range of sources,[32] and large population epidemiological studies assessing acute exposures have found links between the DTT assay-measured OP and adverse cardiorespiratory effects,[23,34] comparisons of OP per particle mass (OP^{DTT}_m) from this study to that of ambient aerosols (e.g., $PM_{2.5}$) provide insights into understanding the measured 3D printer particle DTT activity levels. For this analysis, the particle concentrations in the extracted 3D printer particle solutions were in the range of those of ambient air samples.[29]

Ambient $PM_{2.5}$ OP^{DTT}_m varied from about 25−40 pmol/min/μg based on data from a range of sites in Atlanta (Figure 3A). In general, all 3D printer-emitted particle samples showed relatively lower OP^{DTT}_m than ambient $PM_{2.5}$ (Figure 3A). Estimates of OP^{DTT}_m in emissions from incomplete combustion (e.g., diesel engine exhaust and biomass burning) were even higher (50−150 pmol/min/μg).[32] However, exposure concentrations may be much higher than typical ambient $PM_{2.5}$ levels during printing, especially in poorly ventilated spaces or in close proximity to the operating printer.

Although OP^{DTT}_m provides some indication of aerosol hazard levels, potential adverse health effects depend on actual exposure levels, or particle concentrations. For OP, the equivalent to concentration is OP normalized to the volume of air sampled (OP^{DTT}_v, nmol/min/m^3), which in turn is related to particle emission rates and degree of subsequent dilution (Table S3). Figure 3B shows OP^{DTT}_v for particle levels within the well-mixed 1 m^3 test chamber. Because the chamber setup (i.e., dilution rate) was identical for all the tests in this study, OP^{DTT}_v for the different filaments can be compared directly. Because of the orders of magnitudes lower particle emissions from the *PLA* filament (Table S1 and Figure S3), *PLA* had the lowest OP^{DTT}_v. *ABS* OP^{DTT}_v was factors of 60−100 higher than that of *PLA*, and OP^{DTT}_v of *Nylon* was at the low end of *ABS* but about 25 times as that of *PLA*.

Potential exposure levels were also estimated using an exposure model[14] for three different indoor environmental scenarios (details in Supporting Information section S5). For each scenario, OP^{DTT}_v was calculated by OP^{DTT}_m (pmol/min/μg) × predicted particle concentration (μg/m^3). Among the three scenarios, school setting had the lowest OP^{DTT}_v because of a larger space and better ventilation (Table S4), and residential home setting had the smallest space and lowest ventilation (Table S4), giving the highest OP^{DTT}_v (Figure 4). This indicates the importance of dilution as a way of reducing exposures.

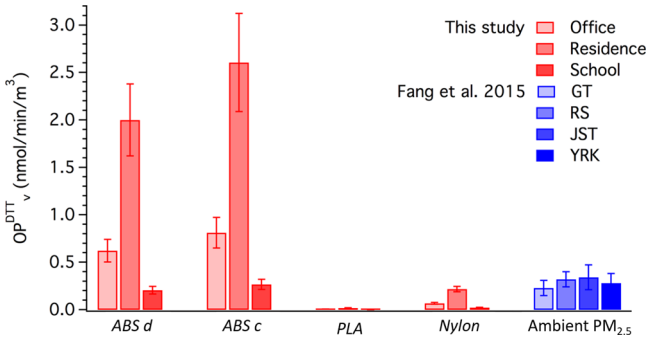

Figure 4. OP^{DTT}_v calculated using OP^{DTT}_m measured in this study and model predicted 3D printer particle concentrations in office, residence, and school settings for each filament (*ABS d*, *ABS c*, *PLA*, *Nylon*, in red), compared to previous ambient air $PM_{2.5}$ study[29] at various monitoring sites in the metropolitan Atlanta region (GT, RS, JST, YRK, in blue, see Figure 3 caption). The error bar for this study represents standard deviation of each group because of measurements (n = 3 for each filament sample); error bar for Fang et al.[29] represents standard deviation of data for each monitoring site.

These indoor scenarios can also be compared to ambient OP levels. Estimated exposure levels to ABS filament emissions in office and residential settings had OP^{DTT}_v higher than ambient $PM_{2.5}$, and the school estimated exposure was comparable to ambient data (Figure 4). *PLA* and *Nylon* showed much lower OP^{DTT}_v than ambient PM OP^{DTT}_v because of their much lower emission levels, except for *Nylon* in the residential setting (Figure 4). The length of exposure time is also important, because printing complex objects can take hours or longer, overall exposures to 3D-printed particles could be substantial. This analysis emphasizes the importance of understanding and minimizing actual exposure concentrations, which depend on conditions, could vary by orders of magnitude.

It is surprising that the chemical assay-measured DTT activities were similar for *PLA* and *ABS* filaments, although the composition analysis showed that they are largely chemically different. A limitation in our analysis is that the chemical analysis of the particle considered the overall aerosol

DOI: 10.1021/acs.est.9b04168
Environ. Sci. Technol. 2019, 53, 12054−12061

composition, whereas because these particles are insoluble, only the surface compounds of the particles will interact with DTT. Also, both biological and chemical analyses showed toxic responses from 3D printer-emitted particles at our sample concentrations; there was a difference that the *PLA*-emitted particles were more toxic than *ABS d* by biological analysis (Figure 2) but similar for the chemical analysis (Figure 3A). Toxicity responses may not only be associated with the doses and chemical properties of the particles, but other properties like particle sizes and their ability to penetrate cells and tissues, cell lines, and interaction mechanism may also be important.[28,46,47] This can affect the biological toxicity responses but have less effect on the chemical assays. For example, NPs were found to be more toxic than larger-sized particles of the same material and dose,[48] causing inflammation and oxidative stress.[49] SEM showed that *PLA*-emitted particles were smaller than *ABS d* in average size, which indicated that they are potentially easier to be transported into cells and further causing cell damage. On the other hand, because of the large difference of emission levels (*PLA* particle mass yield about 2 orders of magnitudes lower than *ABS*, Table S3), the PLA material may not be as toxic as the ABS material when considering overall exposure. Gümperlein et al. found no acute effect on nasal secretion or urine inflammatory markers after 1 h print with ABS or PLA, while the exhaled nitric oxide, which indicates potential airway inflammation or allergy, was higher for printing with ABS than PLA.[50]

Overall, this study indicates that particles emitted from 3D printers with ABS, PLA, and nylon filaments have the potential to induce adverse health impacts, while the chemical compositions of the particles may be associated with raw filament material or additives. Our observed increases in cell death, oxidative stress/OP, and inflammatory responses by both biological and chemical assays are mechanisms that potentially negatively affect lung function, which may increase the risk of respiratory disorders and complications. In this study, toxicity levels of emitted particles were assessed; however, actual exposure study assessments are required to determine the severity of the responses, if any, because exposure depends on many factors that need to be considered, including the conditions under which the printer operates (e.g., size of space and degree of ventilation and turbulence), a person's proximity to the printer, and the duration of exposure. From this analysis, we recommend to lower particle exposures by selecting filaments with low particle emissions, such as PLA, operating the printer(s) in well-ventilated spaces, and limiting time spent in close proximity to operating printer(s).

■ ASSOCIATED CONTENT

Supporting Information

The Supporting Information is available free of charge on the ACS Publications website at DOI: 10.1021/acs.est.9b04168.

Estimation of particle concentrations in liquids; particle characterizations including chamber measurement, chemical composition, and SEM; particle toxicity results including in vitro cell viability, cell death type, intracellular ROS generation assays, in vivo mice exposures, and total DTT assay; exposure model specification (PDF)

■ AUTHOR INFORMATION

Corresponding Author

*E-mail: rweber@eas.gatech.edu.

ORCID

Qian Zhang: 0000-0001-5004-3058
Yinon Rudich: 0000-0003-3149-0201
Jenny P. S. Wong: 0000-0002-8729-8166

Author Contributions

⊥Q.Z. and M.P. contributed equally to this work.

Notes

The authors declare no competing financial interest.

■ ACKNOWLEDGMENTS

This work was funded by the Chemical Safety and Human Health Research Program of Underwriters Laboratories Inc. The SEM analysis was conducted at the Irving and Cherna Moskowitz Center for Nano and BioNano Imaging (Weizmann Institute). Y.R. acknowledges support by Astrachan Olga Klein.

■ REFERENCES

(1) Horvath, J. A Brief History of 3D Printin. *Mastering 3D Printing*; Apress: Berkeley, CA, 2014; pp 3−10.
(2) Kreiger, M.; Pearce, J. M. Environmental Impacts of Distributed Manufacturing from 3-D Printing of Polymer Components and Products. *MRS Proc.* **2013**, *1492*, 85.
(3) Azimi, P.; Zhao, D.; Pouzet, C.; Crain, N. E.; Stephens, B. Emissions of Ultrafine Particles and Volatile Organic Compounds from Commercially Available Desktop Three-Dimensional Printers with Multiple Filaments. *Environ. Sci. Technol.* **2016**, *50*, 1260−1268.
(4) Floyd, E. L.; Wang, J.; Regens, J. L. Fume Emissions from a Low-Cost 3-D Printer with Various Filaments. *J. Occup. Environ. Hyg.* **2017**, *14*, 523−533.
(5) Yi, J.; LeBouf, R. F.; Duling, M. G.; Nurkiewicz, T.; Chen, B. T.; Schwegler-Berry, D.; Virji, M. A.; Stefaniak, A. B. Emission of Particulate Matter from a Desktop Three-Dimensional (3D) Printer. *J. Toxicol. Environ. Health, Part A* **2016**, *79*, 453−465.
(6) Kim, Y.; Yoon, C.; Ham, S.; Park, J.; Kim, S.; Kwon, O.; Tsai, P.-J. Emissions of Nanoparticles and Gaseous Material from 3D Printer Operation. *Environ. Sci. Technol.* **2015**, *49*, 12044−12053.
(7) Zhang, Q.; Wong, J. P. S.; Davis, A. Y.; Black, M. S.; Weber, R. J. Characterization of Particle Emissions from Consumer Fused Deposition Modeling 3D Printers. *Aerosol Sci. Technol.* **2017**, *51*, 1275−1286.
(8) Deng, Y.; Cao, S.-J.; Chen, A.; Guo, Y. The Impact of Manufacturing Parameters on Submicron Particle Emissions from a Desktop 3D Printer in the Perspective of Emission Reduction. *Build. Environ.* **2016**, *104*, 311−319.
(9) Gu, J.; Wensing, M.; Uhde, E.; Salthammer, T. Characterization of Particulate and Gaseous Pollutants Emitted during Operation of a Desktop 3D Printer. *Environ. Int.* **2019**, *123*, 476−485.
(10) Unwin, J.; Coldwell, M. R.; Keen, C.; McAlinden, J. J. Airborne emissions of carcinogens and respiratory sensitizers during thermal processing of plastics. *Ann. Occup. Hyg.* **2013**, *57*, 399−406.
(11) Pirela, S. V.; Pyrgiotakis, G.; Bello, D.; Thomas, T.; Castranova, V.; Demokritou, P. Development and Characterization of an Exposure Platform Suitable for Physico-Chemical, Morphological and Toxicological Characterization of Printer-Emitted Particles (PEPs). *Inhalation Toxicol.* **2014**, *26*, 400−408.
(12) Stefaniak, A. B.; LeBouf, R. F.; Duling, M. G.; Yi, J.; Abukabda, A. B.; McBride, C. R.; Nurkiewicz, T. R. Inhalation Exposure to Three-Dimensional Printer Emissions Stimulates Acute Hypertension and Microvascular Dysfunction. *Toxicol. Appl. Pharmacol.* **2017**, *335*, 1−5.

(13) Stefaniak, A. B.; LeBouf, R. F.; Yi, J.; Ham, J.; Nurkewicz, T.; Schwegler-Berry, D. E.; Chen, B. T.; Wells, J. R.; Duling, M. G.; Lawrence, R. B.; et al. Characterization of Chemical Contaminants Generated by a Desktop Fused Deposition Modeling 3-Dimensional Printer. *J. Occup. Environ. Hyg.* **2017**, *14*, 540−550.
(14) Davis, A. Y.; Zhang, Q.; Wong, J. P. S.; Weber, R. J.; Black, M. S. Characterization of Volatile Organic Compound Emissions from Consumer Level Material Extrusion 3D Printers. *Build. Environ.* **2019**, *160*, 106209.
(15) Steinle, P. Characterization of Emissions from a Desktop 3D Printer and Indoor Air Measurements in Office Settings. *J. Occup. Environ. Hyg.* **2016**, *13*, 121−132.
(16) Vance, M. E.; Pegues, V.; Van Montfrans, S.; Leng, W.; Marr, L. C. Aerosol Emissions from Fuse-Deposition Modeling 3D Printers in a Chamber and in Real Indoor Environments. *Environ. Sci. Technol.* **2017**, *51*, 9516−9523.
(17) Zontek, T. L.; Ogle, B. R.; Jankovic, J. T.; Hollenbeck, S. M. An Exposure Assessment of Desktop 3D Printing. *J. Chem. Health Saf.* **2017**, *24*, 15−25.
(18) Stabile, L.; Scungio, M.; Buonanno, G.; Arpino, F.; Ficco, G. Airborne Particle Emission of a Commercial 3D Printer: The Effect of Filament Material and Printing Temperature. *Indoor Air* **2017**, *27*, 398−408.
(19) Oberdörster, G.; Oberdörster, E.; Oberdörster, J. Nanotoxicology: An Emerging Discipline Evolving from Studies of Ultrafine Particles. *Environ. Health Perspect.* **2005**, *113*, 823−839.
(20) Li, N.; Sioutas, C.; Cho, A.; Schmitz, D.; Misra, C.; Sempf, J.; Wang, M.; Oberley, T.; Froines, J.; Nel, A. Ultrafine Particulate Pollutants Induce Oxidative Stress and Mitochondrial Damage. *Environ. Health Perspect.* **2003**, *111*, 455−460.
(21) Pardo, M.; Xu, F.; Shemesh, M.; Qiu, X.; Barak, Y.; Zhu, T.; Rudich, Y. Nrf2 Protects against Diverse PM2.5 Components-Induced Mitochondrial Oxidative Damage in Lung Cells. *Sci. Total Environ.* **2019**, *669*, 303−313.
(22) Hussain, S.; Boland, S.; Baeza-Squiban, A.; Hamel, R.; Thomassen, L. C. J.; Martens, J. A.; Billon-Galland, M. A.; Fleury-Feith, J.; Moisan, F.; Pairon, J.-C.; et al. Oxidative Stress and Proinflammatory Effects of Carbon Black and Titanium Dioxide Nanoparticles: Role of Particle Surface Area and Internalized Amount. *Toxicology* **2009**, *260*, 142−149.
(23) Abrams, J. Y.; Weber, R. J.; Klein, M.; Samat, S. E.; Chang, H. H.; Strickland, M. J.; Verma, V.; Fang, T.; Bates, J. T.; Mulholland, J. A.; et al. Associations between Ambient Fine Particulate Oxidative Potential and Cardiorespiratory Emergency Department Visits. *Environ. Health Perspect.* **2017**, *125*, 107008.
(24) Li, N.; Xia, T.; Nel, A. E. The Role of Oxidative Stress in Ambient Particulate Matter-Induced Lung Diseases and Its Implications in the Toxicity of Engineered Nanoparticles. *Free Radical Biol. Med.* **2008**, *44*, 1689−1699.
(25) Ayres, J. G.; Borm, P.; Cassee, F. R.; Castranova, V.; Donaldson, K.; Ghio, A.; Harrison, R. M.; Hider, R.; Kelly, F.; Kooter, I. M.; et al. Evaluating the Toxicity of Airborne Particulate Matter and Nanoparticles by Measuring Oxidative Stress Potential-A Workshop Report and Consensus Statement. *Inhalation Toxicol.* **2008**, *20*, 75−99.
(26) Keenan, C. R.; Goth-Goldstein, R.; Lucas, D.; Sedlak, D. L. Oxidative Stress Induced by Zero-Valent Iron Nanoparticles and Fe(II) in Human Bronchial Epithelial Cells. *Environ. Sci. Technol.* **2009**, *43*, 4555−4560.
(27) Pardo, M.; Shafer, M. M.; Rudich, A.; Schauer, J. J.; Rudich, Y. Single Exposure to near Roadway Particulate Matter Leads to Confined Inflammatory and Defense Responses: Possible Role of Metals. *Environ. Sci. Technol.* **2015**, *49*, 8777−8785.
(28) Peixoto, M. S.; de Oliveira Galvão, M. F.; Batistuzzo de Medeiros, S. R. Cell Death Pathways of Particulate Matter Toxicity. *Chemosphere* **2017**, *188*, 32−48.
(29) Fang, T.; Verma, V.; Guo, H.; King, L. E.; Edgerton, E. S.; Weber, R. J. A Semi-Automated System for Quantifying the Oxidative Potential of Ambient Particles in Aqueous Extracts Using the Dithiothreitol (DTT) Assay: Results from the Southeastern Center for Air Pollution and Epidemiology (SCAPE). *Atmos. Meas. Tech.* **2015**, *8*, 471−482.
(30) Fang, T.; Verma, V.; Bates, J. T.; Abrams, J.; Klein, M.; Strickland, M. J.; Sarnat, S. E.; Chang, H. H.; Mulholland, J. A.; Tolbert, P. E.; et al. Oxidative Potential of Ambient Water-Soluble $PM_{2.5}$ in the Southeastern United States: Contrasts in Sources and Health Associations between Ascorbic Acid (AA) and Dithiothreitol (DTT) Assays. *Atmos. Chem. Phys.* **2016**, *16*, 3865−3879.
(31) Sauvain, J.-J.; Rossi, M. J.; Riediker, M. Comparison of Three Acellular Tests for Assessing the Oxidation Potential of Nanomaterials. *Aerosol Sci. Technol.* **2013**, *47*, 218−227.
(32) Shiraiwa, M.; Ueda, K.; Pozzer, A.; Lammel, G.; Kampf, C. J.; Fushimi, A.; Enami, S.; Arangio, A. M.; Fröhlich-Nowoisky, J.; Fujitani, Y.; et al. Aerosol Health Effects from Molecular to Global Scales. *Environ. Sci. Technol.* **2017**, *51*, 13545−13567.
(33) Yang, A.; Janssen, N. A. H.; Brunekreef, B.; Cassee, F. R.; Hoek, G.; Gehring, U. Children's Respiratory Health and Oxidative Potential of PM2.5: The PIAMA Birth Cohort Study. *Occup. Environ. Med.* **2016**, *73*, 154−160.
(34) Bates, J. T.; Weber, R. J.; Abrams, J.; Verma, V.; Fang, T.; Klein, M.; Strickland, M. J.; Sarnat, S. E.; Chang, H. H.; Mulholland, J. A.; et al. Reactive Oxygen Species Generation Linked to Sources of Atmospheric Particulate Matter and Cardiorespiratory Effects. *Environ. Sci. Technol.* **2015**, *49*, 13605−13612.
(35) Weichenthal, S. A.; Lavigne, E.; Evans, G. J.; Godri Pollitt, K. J.; Burnett, R. T. Fine Particulate Matter and Emergency Room Visits for Respiratory Illness. Effect Modification by Oxidative Potential. *Am. J. Respir. Crit. Care Med.* **2016**, *194*, 577−586.
(36) Weichenthal, S.; Crouse, D. L.; Pinault, L.; Godri-Pollitt, K.; Lavigne, E.; Evans, G.; van Donkelaar, A.; Martin, R. V.; Burnett, R. T. Oxidative Burden of Fine Particulate Air Pollution and Risk of Cause-Specific Mortality in the Canadian Census Health and Environment Cohort (CanCHEC). *Environ. Res.* **2016**, *146*, 92−99.
(37) ASTM International. Designation: D6670—13. *Standard Practice for Full-Scale Chamber Determination of Volatile Organic Emissions from Indoor Materials/Products*. 2013.
(38) Zhang, Q.; Sharma, G.; Wong, J. P. S.; Davis, A. Y.; Black, M. S.; Biswas, P.; Weber, R. J. Investigating Particle Emissions and Aerosol Dynamics from a Consumer Fused Deposition Modeling 3D Printer with a Lognormal Moment Aerosol Model. *Aerosol Sci. Technol.* **2018**, *52*, 1099−1111.
(39) Ng, N. L.; Herndon, S. C.; Trimborn, A.; Canagaratna, M. R.; Croteau, P. L.; Onasch, T. B.; Sueper, D.; Worsnop, D. R.; Zhang, Q.; Sun, Y. L.; et al. An Aerosol Chemical Speciation Monitor (ACSM) for Routine Monitoring of the Composition and Mass Concentrations of Ambient Aerosol. *Aerosol Sci. Technol.* **2011**, *45*, 780−794.
(40) Drewnick, F.; Hings, S. S.; DeCarlo, P.; Jayne, J. T.; Gonin, M.; Fuhrer, K.; Weimer, S.; Jimenez, J. L.; Demerjian, K. L.; Borrmann, S.; et al. A New Time-of-Flight Aerosol Mass Spectrometer (TOF-AMS)-Instrument Description and First Field Deployment. *Aerosol Sci. Technol.* **2005**, *39*, 637−658.
(41) DeCarlo, P. F.; Kimmel, J. R.; Trimborn, A.; Northway, M. J.; Jayne, J. T.; Aiken, A. C.; Gonin, M.; Fuhrer, K.; Horvath, T.; Docherty, K. S.; et al. Field-Deployable, High-Resolution, Time-of-Flight Aerosol Mass Spectrometer. *Anal. Chem.* **2006**, *78*, 8281−8289.
(42) Pardo, M.; Shuster-Meiseles, T.; Levin-Zaidman, S.; Rudich, A.; Rudich, Y. Low Cytotoxicity of Inorganic Nanotubes and Fullerene-Like Nanostructures in Human Bronchial Epithelial Cells: Relation to Inflammatory Gene Induction and Antioxidant Response. *Environ. Sci. Technol.* **2014**, *48*, 3457−3466.
(43) Cho, A. K.; Sioutas, C.; Miguel, A. H.; Kumagai, Y.; Schmitz, D. A.; Singh, M.; Eiguren-Fernandez, A.; Froines, J. R. Redox Activity of Airborne Particulate Matter at Different Sites in the Los Angeles Basin. *Environ. Res.* **2005**, *99*, 40−47.
(44) Gao, D.; Fang, T.; Verma, V.; Zeng, L.; Weber, R. J. A Method for Measuring Total Aerosol Oxidative Potential (OP) with the Dithiothreitol (DTT) Assay and Comparisons between an Urban and

DOI: 10.1021/acs.est.9b04168
Environ. Sci. Technol. 2019, 53, 12054−12061

Roadside Site of Water-Soluble and Total OP. *Atmos. Meas. Tech.* **2017**, *10*, 2821−2835.
(45) Stein, S. E. Mass Spectra. *NIST Chemistry WebBook*, NIST Standard Reference Database Number 69, 2016.
(46) Grass, R. N.; Limbach, L. K.; Athanassiou, E. K.; Stark, W. J. Exposure of Aerosols and Nanoparticle Dispersions to in Vitro Cell Cultures: A Review on the Dose Relevance of Size, Mass, Surface and Concentration. *J. Aerosol Sci.* **2010**, *41*, 1123−1142.
(47) Perrone, M. G.; Gualtieri, M.; Consonni, V.; Ferrero, L.; Sangiorgi, G.; Longhin, E.; Ballabio, D.; Bolzacchini, E.; Camatini, M. Particle Size, Chemical Composition, Seasons of the Year and Urban, Rural or Remote Site Origins as Determinants of Biological Effects of Particulate Matter on Pulmonary Cells. *Environ. Pollut.* **2013**, *176*, 215−227.
(48) Oberdorster, G.; Ferin, J.; Lehnert, B. E. Correlation between Particle Size, in Vivo Particle Persistence, and Lung Injury. *Environ. Health Perspect.* **1994**, *102*, 173−179.
(49) Nel, A.; Xia, T.; Mädler, L.; Li, N. Toxic Potential of Materials at the Nanolevel. *Science* **2006**, *311*, 622−627.
(50) Gümperlein, I.; Fischer, E.; Dietrich-Gümperlein, G.; Karrasch, S.; Nowak, D.; Jörres, R. A.; Schierl, R. Acute Health Effects of Desktop 3D Printing (Fused Deposition Modeling) Using Acrylonitrile Butadiene Styrene and Polylactic Acid Materials: An Experimental Exposure Study in Human Volunteers. *Indoor Air* **2018**, *28*, 611−623.

DOI: 10.1021/acs.est.9b04168
Environ. Sci. Technol. 2019, 53, 12054−12061